

Magnetic and transport studies of pure V_2O_3 under pressure

S. A. Carter,* T. F. Rosenbaum, M. Lu, and H. M. Jaeger

The James Franck Institute and Department of Physics, The University of Chicago, Chicago, Illinois 60637

P. Metcalf, J. M. Honig, and J. Spalek

Department of Chemistry, Purdue University, West Lafayette, Indiana 47907

(Received 29 November 1993)

We report a systematic study of the resistivity and magnetic susceptibility of pure V_2O_3 , the original Mott-Hubbard system at half filling, for pressures $0 \leq P \leq 25$ kbar and temperatures $0.35 \leq T \leq 300$ K. We also study $(V_{0.99}Ti_{0.01})_2O_3$ under pressure in order to elucidate the role of disorder on a metal-insulator transition in the highly correlated limit. Despite the low level of doping, we find that the two systems are very different. We observe a conventional collapsing of the Mott-Hubbard gap only for stoichiometric V_2O_3 ; the Ti disorder stabilizes the long-range antiferromagnetic order and a magnetic Slater gap. Moreover, we discover different P - T phase diagrams for the two systems, with a decoupling of the charge and spin degrees of freedom at the approach to the $T=0$, pressure-driven metal-insulator transition in pure V_2O_3 .

INTRODUCTION

One of the most intriguing aspects of the Mott-Hubbard metal-insulator transition¹ (MIT) is the mix of enhanced electron interactions, strong spin fluctuations, unusual magnetic order, and dopant disorder. The interplay of these elements is not only of interest for Mott-Hubbard transition metal oxides, but bears on the ground-state properties of the high- T_c cuprate superconductors and the heavy fermion compounds. This recognition has led to a flurry of Mott-Hubbard models in dimensions from 1 to infinity.²⁻⁴ The infinite-dimension approach² provides a means to match the Mott-Hubbard treatment of the insulator at half filling to the Brinkman-Rice picture⁵ of the highly correlated metal. The two-dimensional (2D) t - J Hubbard models predict an incommensurate spiral spin-density wave phase³ which is akin to recent neutron-scattering results on metallic $V_{2-y}O_3$.⁶ In addition, a diverging effective mass, first predicted by Brinkman and Rice, has been discovered in the past few months as the MIT is approached from both the spiral antiferromagnetic⁷ and paramagnetic metal states⁸ of Mott-Hubbard materials. Despite these successes, our understanding of the Mott-Hubbard problem is incomplete, and theories have gone largely untested because few detailed experimental studies of the appropriate systems exist.

One of the major complications is the role that band filling and the associated dopant disorder plays in Mott-Hubbard systems. We now know that doping has different ramifications for the phase diagram and the underlying physical state than the other conventional method for crossing the MIT, hydrostatic pressure.^{7,9} In particular, doping introduces additional carriers, localization effects, and, often, magnetic impurities. By comparison, hydrostatic pressure primarily affects the ratio of the bandwidth B to the intra-atomic repulsion U . Most experiments in the field have been performed as a function of band filling rather than pressure and, therefore, rarely can be applied directly to theories that do not address complications beyond a parametrization in terms of

B/U . This limitation is particularly true for V_2O_3 , which has served as the classic example of the Mott-Hubbard transition and the Brinkman-Rice correlated metal.^{5,10} A number of very careful studies have focused on the MIT in vanadium sesquioxide as functions of vanadium vacancy concentration and Ti and Cr substitution for V;¹¹⁻¹³ however, only a few experiments exist that study the MIT as it is approached with pressure.^{9,10,14,15} In particular, no systematic study over a full range of temperature T and pressure P has been performed on the benchmark half-filled case, stoichiometric V_2O_3 .

In this paper we rectify this oversight by studying the resistivity and magnetic susceptibility of pure V_2O_3 under pressure for $0.35 \leq T \leq 300$ K. In particular, we probe the system right near the MIT and find unusual behavior not previously reported. We also study $(V_{0.99}Ti_{0.01})_2O_3$ under pressure, in order to elucidate the role of disorder in the same Mott-Hubbard material. Despite the low level of doping, we find that the two systems are very different. We observe a conventional collapse of the Mott-Hubbard gap only for stoichiometric V_2O_3 ; the Ti disorder, or doping with minority spin- $\frac{1}{2}$ moments, stabilizes the long-range antiferromagnetic order and a magnetic Slater gap,¹⁶ and leads to Mott variable range hopping (VRH) in low-temperature transport. Finally, we discover different phase diagrams for the two systems, with the existence of a previously unobserved paramagnetic insulating phase in a sliver of the P - T diagram of pure V_2O_3 .

EXPERIMENTAL TECHNIQUES

Single crystals of typical size 1 cm^3 were prepared at Purdue University. $(V_{0.9}Ti_{0.01})_2O_3$ was grown from melt by the Reed Tri-arc technique, and pure V_2O_3 crystals were grown using a skull melter. Thin slices were then annealed in a H_2 atmosphere until rendered stoichiometric.¹⁷ The stoichiometry of the samples was determined with use of thermogravimetric analysis.¹⁸ Resistivity data were taken on several different batches of both samples to ensure sample homogeneity and repeatability.

bility. Both sets of samples showed high MIT temperatures [141 K for $(V_{0.99}Ti_{0.01})_2O_3$ and 156 K for V_2O_3 taken upon cooling] with sharp transition widths (< 0.5 K), and metallic resistivities ($\rho = 10^{-6}$ to 10^{-4} Ω cm) indicative of clean single-crystal material.

The need for resistivity and susceptibility data for pressures up to 25 kbar motivated the design of a special BeCu pressure clamp cell. The cell is similar to standard designs; however, the pressure cell bore (6 mm) and surrounding pieces were made of tungsten carbide inserts to allow for repeated use to high P without deformation of the BeCu. The cell dimensions (1.25 in. diam \times 2.75 in. length) were designed to fit into a He^3 refrigerator with a 2-in.-bore superconducting magnet. The temperature of the MIT, T_{MI} , in $(V_{0.99}Ti_{0.01})_2O_3$ as a function of pressure was calibrated using the superconducting transition temperature of lead. Since dT_{MI}/dP for $(V_{0.99}Ti_{0.01})_2O_3$ is 5.8 K/kbar, compared to a dT_c/dP for lead of 0.04 K/kbar, $(V_{0.99}Ti_{0.01})_2O_3$ proved to be a more sensitive manometer.¹⁴ Our pressures were accurate to ± 0.2 kbar below 15 kbar, where we were able to use the $(V_{0.99}Ti_{0.01})_2O_3$ manometer, and to ± 0.5 kbar above 15 kbar. In order to maintain hydrostatic conditions at high pressures, we used silicone oil as the pressure medium. Although it freezes at room temperature at approximately 10 kbar, the solid remains an isotropically deformable glass. We checked that the pressure remained hydrostatic by monitoring the width of the resistive transition of the $(V_{0.99}Ti_{0.01})_2O_3$ manometer and found that pressure inhomogeneities were always less than 0.5 kbar over a distance of 5 mm.

Our transport measurements were all performed in the frequency-independent and Ohmic limits. We used a four-probe 16-Hz ac lock-in technique at low resistance, and a four-probe dc technique above 100 $k\Omega$. Particular care was needed for preparing the stoichiometric V_2O_3 samples since we found that damaged surface layers shorted out the bulk resistivity in the insulator. Our results for stoichiometric V_2O_3 sanded and etched in boiling HCl for 1/2 h agreed with the results on freshly annealed samples. Electrical leads were attached to freshly etched samples of typical dimensions $1 \times 1 \times 3$ mm³ with the use of silver paint, with contact resistances always less than a few Ohms in the metal.

We measured concurrently the magnetic susceptibility of the crystals employing a standard inductance bridge technique. The ac field generated by the primary coil varied with experiment but was always less than 3 G; all results are reported in the magnetic-field and frequency-independent regimes. The secondary and primary coils located inside the pressure cell were wound with 1-mil copper wire to maximize the number of turns per unit length. The temperature-dependent background proved to be small since a 1-mm-thick Teflon bucket effectively isolated the primary and secondary coils inside the bucket from any contribution from the WC or BeCu. The remaining background, at most 30%, was measured independently and subtracted from the results. We used a commercial superconducting quantum interference device (SQUID) magnetometer to perform the ambient pressure magnetization measurements and to calibrate

the ac coils. We estimate the absolute error in the susceptibility to be less than $\pm 0.1 \times 10^{-3}$ emu/mol V.

RESULTS

We plot in Fig. 1 the resistivity $\rho(T)$ for $(V_{0.99}Ti_{0.01})_2O_3$ for a series of pressures P . The temperature hysteresis remains 11 K at all pressures; for clarity, only the data taken upon cooling are shown. The metallic resistivity at high temperatures is pressure independent to within 20% and increases abruptly by four orders of magnitude at a $T_{MI}(P)$ from the paramagnetic metal to the antiferromagnetic insulator. Down to 20 or 30 K below the transition, the data follow standard activated behavior with $\rho = \rho_0 \exp(\Delta_a/T)$. We find that the activation gap Δ_a (~ 600 K) and the step in the resistivity at the MIT, $\Delta\rho_{MIT}$, change modestly with P , as reported earlier over a much smaller range in pressure.¹⁴ Above 17 kbar, the Ti-doped crystal is driven completely metallic and the gap as well as the $T \rightarrow 0$ resistivity, $\rho(0)$, appear to jump discontinuously.

At low T over the entire pressure range, we observe Mott variable range hopping where $\rho = \rho_1 \exp(T_0/T)^{1/4}$.¹⁹ This behavior reflects the disorder introduced by Ti substitution which serves to trap excess holes in the tail of the lower Hubbard band. The solid lines in Fig. 2 are fits of the data to the Mott VRH form at a series of pressures. In the inset, we graph the VRH characteristic temperature T_0 versus P . We can estimate a localization length α^{-1} ,

$$\alpha^{-1} = [k_B T_0 N(E_F)/16]^{-1/3},$$

where $N(E_F)$ is the density of states at the Fermi level (~ 1 state/V atom).¹⁹ We find $\alpha^{-1} = 0.6$ Å for $P = 0$, which increases only slightly to 0.8 Å as the $T \rightarrow 0$ MIT is approached. Although the system is highly correlated, we do not observe an Efros-Shklovskii $\exp(T_0/T)^{1/2}$ dependence in $\rho(T)$,²⁰ presumably because there are a

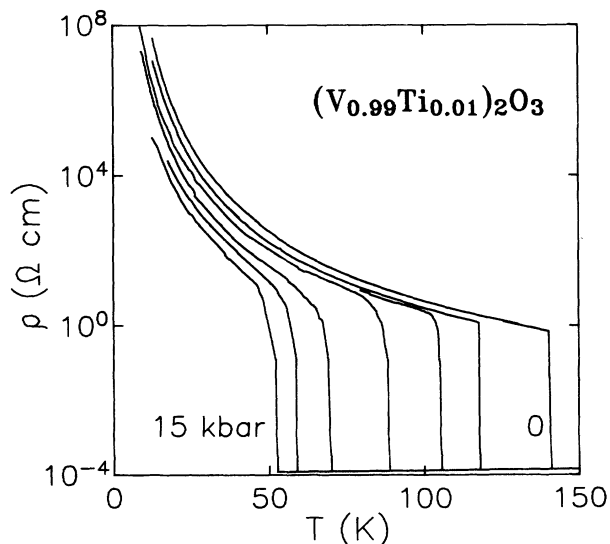


FIG. 1. Resistivity ρ over 12 decades vs temperature T through the metal-insulator transition of Ti-doped V_2O_3 at a series of pressures $P = 0, 4, 6, 9, 12, 14,$ and 15 kbar on cooling.

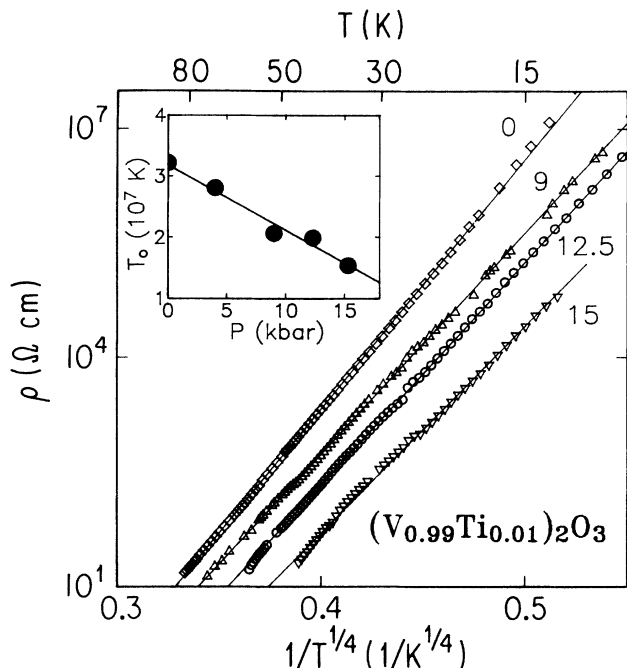


FIG. 2. Substitutional disorder induces Mott variable range hopping, $\rho \sim \exp(T_0/T)^{1/4}$, at low T . Inset: T_0 decreases at the approach to the $T \rightarrow 0$ pressure-driven transition.

sufficient number of thermally excited carriers to screen the Coulomb gap.

We now consider the transport signatures of the ostensibly simpler undoped case, where effects from disorder should not play a role. We plot, in Fig. 3, $\rho(T)$ of pure V_2O_3 taken upon cooling for a series of pressures. The hysteresis associated with the MIT is 11 K at $P=0$, but decreases at higher pressures to 6 K. The behavior of

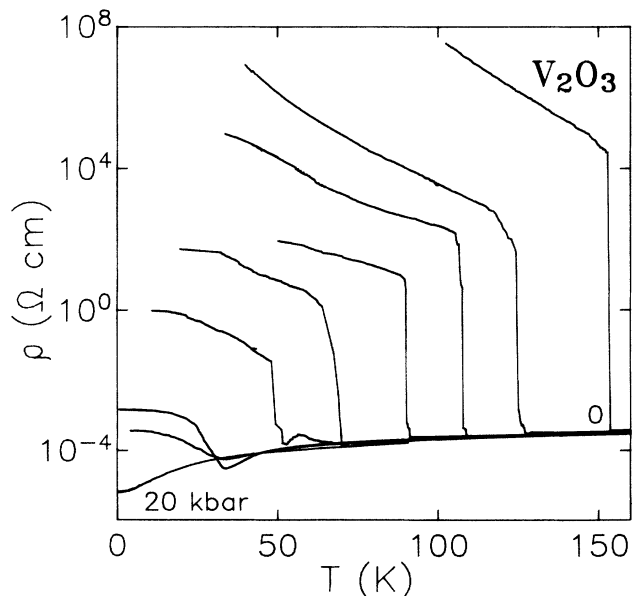


FIG. 3. Resistivity ρ over 14 decades vs temperature T through the metal-insulator transition of pure V_2O_3 at a series of pressures $P=0, 3.5, 6, 9, 11.5, 14, 16, 17,$ and 20 kbar on cooling.

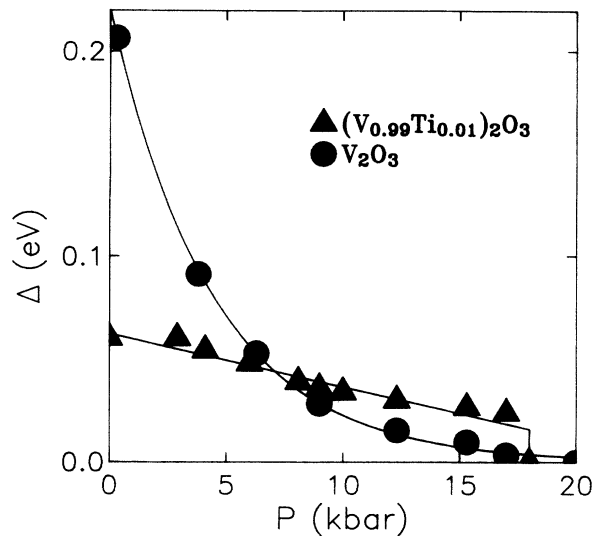


FIG. 4. Activation energy gap Δ in the insulator as a function of pressure P . Δ collapses exponentially with P (line) in V_2O_3 ($P_{MI}=20$ kbar), as expected for a Mott-Hubbard system. Ti doping appears to introduce a magnetic contribution to Δ (see text), leading to a weaker dependence on P and a jump to zero at $P_{MI}=18$ kbar. Here, the line is a guide to the eye.

this system is considerably different than that of $(V_{0.99}Ti_{0.01})_2O_3$. Similar to $(V_{0.99}Ti_{0.01})_2O_3$, activated behavior exists some 20 to 30 K below the MIT. However, at ambient pressure, the jump in resistivity at the MIT ($\Delta\rho_{MIT} \sim 7$ decades) and the activation gap ($\Delta_a \sim 3000$ K) are much larger. Both $\Delta\rho_{MIT}$ and Δ_a decrease rapidly with increasing pressure. They cross below the corresponding values for $(V_{0.99}Ti_{0.01})_2O_3$ at high P and approach zero continuously at the pressure-driven MIT.

We illustrate this relationship in Fig. 4 where we plot the activation gap Δ_a versus pressure for the two samples. The activation gap should be equal to the Mott-Hubbard gap $\Delta = U_{scr} - B$, where U_{scr} is the screened intra-atomic potential (typically a few eV) and B is the bandwidth of the upper and lower Hubbard bands. The narrow bandwidth in highly correlated systems can be very sensitive to P , falling off exponentially with distance: $B \sim \exp(-R/a_B)$, where R is the distance between adjacent V^{3+} sites. The solid curve through the pure V_2O_3 data in Fig. 4 is proportional to $\exp(-P/P_0)$. We can estimate whether the change in Δ with pressure is reasonable, given the change in R with P . The distance between vanadium sites in the plane $R = 2.70$ Å.²¹ If U_{scr} is essentially constant, the gap goes to zero as B changes by 0.2 eV. Hence, R must decrease to 2.65 Å for an initial bandwidth of 1 eV.²² The change of 1.8% is large but feasible given that the V_2O_3 volume and the \hat{a} lattice constant change at room temperature by roughly 1% with 20 kbar of pressure. Hence, the activation energy gap Δ_a in pure V_2O_3 can be described within a Mott-Hubbard framework.

The $(V_{0.99}Ti_{0.01})_2O_3$ data clearly cannot be explained by a simple Mott-Hubbard model. As described by Slater, long-range antiferromagnetic order also can split a half-filled band.¹⁶ The magnetic Slater gap Δ_s depends

directly on the antiferromagnetic exchange term J_{AF} and ordinarily is too small to be observed. However, Δ_a is sufficiently small in $(V_{0.99}Ti_{0.01})_2O_3$ that one might expect to observe Δ_s . The paramagnetic Néel temperature T'_N is related to J_{AF} by

$$k_B T'_N = \frac{1}{3} J_{AF} z S(S+1) = \frac{2}{3} J_{AF} z .$$

Since V_2O_3 is an $S=1$ system, $\Delta_s = \frac{3}{2} k_B T'_N$.¹³ With $T'_N \sim 450$ K,²³ the maximum contribution $\Delta_{smax} \sim 650$ K, which is indeed the magnitude of the gap we observe for the titanium-doped crystals. It is this contribution which keeps Δ_a from decreasing significantly as the MIT is approached. Despite the large Slater term, we still consider $(V_{0.99}Ti_{0.01})_2O_3$ to be a Mott-Hubbard system. The decrease in Δ_a with P reflects the rapidly decreasing Mott-Hubbard contribution to the gap which is of a magnitude similar to Δ_s .

We return to Fig. 3 and to our analysis of $\rho(T)$ for a series of pressures at half filling. As expected, we do not observe Mott VRH in the stoichiometric system. Rather, the resistivity for V_2O_3 follows a subexponential behavior at low T . A number of other MIT systems exhibit this unconventional behavior, the origin of which may range from impurity states in the gap to a temperature-dependent gap, or, as claimed for the related $Ni_{1-x}Co_xS_2$ system, to conduction by small polarons.²⁴ The clean activated behavior in V_2O_3 for $T \leq T_{MI}$ and the sharp transition at ambient pressure make unlikely the existence of significant impurities in our crystals, but the other possibilities remain plausible.

At higher pressures, an additional feature emerges in $\rho(T)$ about 10 K above the MIT. This upturn and local maximum, clearly defined for $6 \leq P \leq 15$ kbar, looks very similar to what is observed in other vanadium oxides, where it is attributed to the formation of an antiferromagnetic metal phase.²⁵ Since the feature is hysteretic, the posited transition from paramagnetic to antiferromagnetic metal would have to be first order, an unusual but not impossible occurrence if the magnetic transition is linked to a structural change. Clearly, the resistivity measurements need to be supplemented with magnetic

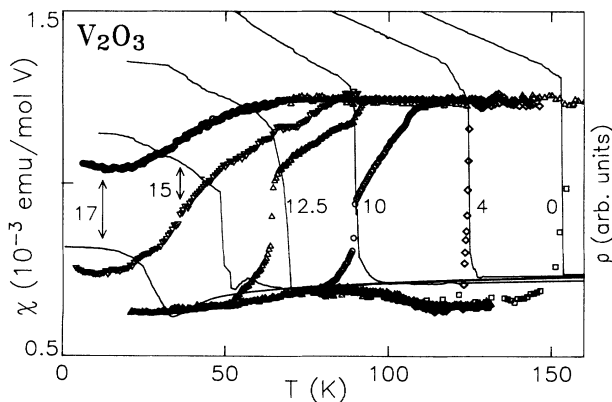


FIG. 5. Magnetic susceptibility $\chi(T)$ (symbols) overlaid on the resistivity $\rho(T)$ (lines) at a series of pressures for pure V_2O_3 . The two decouple for $P \geq 15$ kbar.

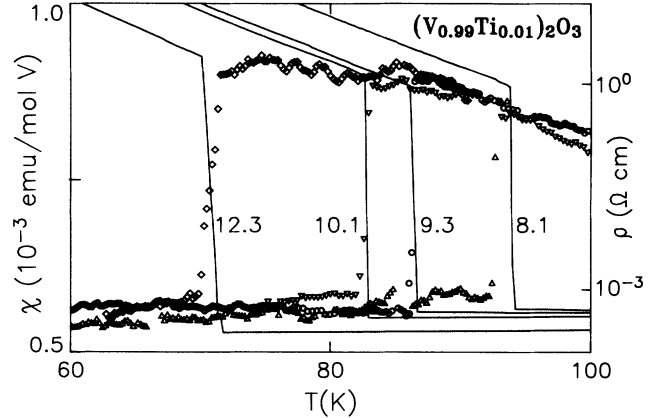


FIG. 6. Analogous plot to Fig. 5 for the doped system. In this case, the spin and charge transitions track at all P .

susceptibility data to get a firmer picture of what is transpiring.

We graph in Fig. 5 the magnetic susceptibility χ of V_2O_3 overlaid on its resistive response. At moderate pressures (< 17 kbar), $\chi(T)$ is hysteretic over the region of change, just like $\rho(T)$, so again for clarity we show only the data taken upon cooling. At $P=0$, we observe a sharp transition in $\chi(T)$, indicating the onset of antiferromagnetism. The transition in χ continues to be sharp at low pressures, but starts to broaden slowly above $P=6$ kbar, even though the resistive transition remains narrow. Comparison to $\chi(T)$ of $(V_{0.99}Ti_{0.01})_2O_3$ (cf. Fig. 6), which remains sharp at all P and is taken in the same pressure cell at the same time, indicates that the broadening cannot be due to pressure inhomogeneities. Moreover, we have checked that the forms of $\chi(T)$ and $\rho(T)$ repeat for three crystals prepared and annealed separately. We note that surface effects are necessarily small because the susceptibility is a bulk measurement.

We observe a small change in the slope of $\rho(T)$ in the metal where $\chi(T)$ starts to decrease, but no corresponding signature in the insulator where $\chi(T)$ has finished evolving. The decrease in χ well above the MIT indicates a broad precursory region where local magnetic order presumably develops, culminating in global antiferromagnetism stabilized by the transition into the insulator.

The total change in the magnetic susceptibility about T_{MI} remains constant for $P < 15$ kbar. At higher pressures, the magnitude of the change in $\chi(T)$ decreases with increasing P , disappearing by 20 kbar. Furthermore, we no longer observe either a sharp drop in $\chi(T)$ indicative of the Néel transition nor any feature in the susceptibility at the upturn and local maximum in $\rho(T)$. This indicates that the resistive feature found roughly 10 K above the jump in $\rho(T)$ depends on the MIT itself and not on the magnetic order (as claimed in the interpretation of transport measurements²⁵ on higher-order members of the Magneli series, V_nO_{2n-1}). Above $P=15$ kbar, the hysteresis in the susceptibility is only a few Kelvins and no longer can be observed by 17 kbar, even though the resistive hysteresis remains over 6 K. We expect that at this point the magnetic order is short range and no longer

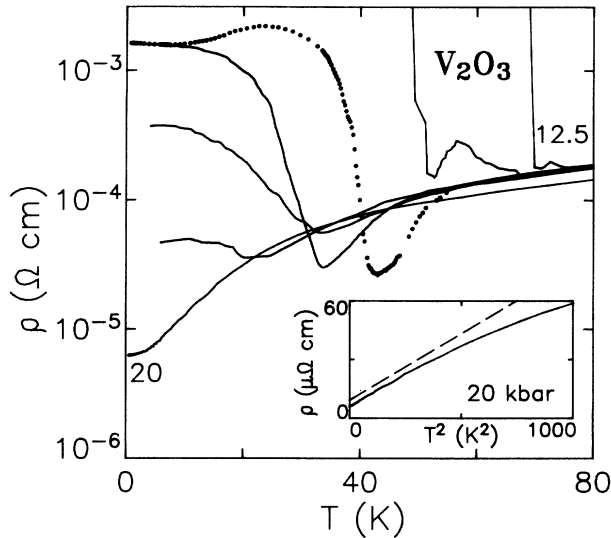


FIG. 7. Transport behavior of pure V_2O_3 in the immediate vicinity of the $T \rightarrow 0$ pressure-driven transition at $P = 12.5, 14, 16, 17, 18,$ and 20 kbar. Hysteresis remains for $P < 20$ kbar: solid lines are taken on cooling, the dotted line at $P = 17$ kbar on warming. Inset: $\rho(T) \sim T^2$ in the highly correlated metal at low T .

tion tied directly to the first-order MIT.

We compare the relationship of $\chi(T)$ and $\rho(T)$ in pure V_2O_3 to the case of $(V_{0.99}Ti_{0.01})_2O_3$ in Fig. 6. Except for a slight change in scale, the magnetic transition is very similar to that of the undoped compound at ambient pressure. At higher P , the similarities end. For $(V_{0.99}Ti_{0.01})_2O_3$, the magnitude of the change in $\chi(T)$ at T_{MI} remains constant and it faithfully tracks the resistive transition. There is no precursory region or indication of local moment formation; the spin and charge degrees of freedom always are linked.

We focus last on the behavior of pure V_2O_3 near the $T \rightarrow 0$ MIT boundary, as shown in Fig. 7. The data at $P = 17$ and 20 kbar are plotted down to $T = 0.35$ K. At 17 kbar, there is a continuous two-decade increase in the resistivity with decreasing temperature, but no discontinuous step characteristic of a first-order MIT. Nonetheless, the apparent transition remains markedly hysteretic. On cooling (solid lines), $\rho(T)$ continues to rise with decreasing T , indicative of insulatinglike behavior, but tends toward saturation at the lowest temperatures we reach. The data taken upon warming (dotted line at $P = 17$ kbar) have a clear maximum at 25 K. This unusual behavior was reproduced for a number of different crystals of pure V_2O_3 , and a similar response under pressure has been observed in the related system $PrNiO_3$.²⁶ At the same time, the susceptibility (Fig. 5) shows little temperature dependence above background at the approach to the $T \rightarrow 0$ MIT boundary, and it displays no sharp features which would constitute a magnetic transition. In addition, we have found that $\rho(T)$ is essentially insensitive to applied magnetic field up to at least 8 T.

Possible explanations for the unusual transport behavior run the gamut from Kondo insulators, as in the heavy fermion compounds, to excitonic insulators to

semimetals, as in the Mott-Hubbard system NiS . What we wish to stress, however, is that this is a region of the phase diagram where magnetism no longer plays a pivotal role and where it may be possible to deconvolute the effects of the electronic correlations at the MIT.

By 20 kbar, the system is completely metallic and $\rho(T)$ is no longer hysteretic. There is neither an antiferromagnetic nor a superconducting ground state down to 350 mK. We graph, in the inset to Fig. 7 ρ versus T^2 at $P = 20$ kbar. The strongly enhanced electron-electron interactions give rise to the T^2 behavior in the $T \rightarrow 0$ limit, but, as with the doped samples, the fit starts to deviate around 20 K. The slope is $6.0 \pm 0.2 \times 10^{-8} \Omega \text{ cm/K}^2$, comparable to the value of $5.8 \times 10^{-8} \Omega \text{ cm/K}^2$ reported by McWhan *et al.*¹⁰ for V_2O_3 under 26 kbar of pressure. The resistivity in the $T \rightarrow 0$ limit, $\rho(0)$, is much smaller than for the doped systems ($6 \mu\Omega \text{ cm}$ compared to $200 \mu\Omega \text{ cm}$). This could be expected simply in terms of impurity-scattering contributions to the resistivity; however, we find that $\rho(0)$ is essentially constant with doping once the system is stabilized metallic with V vacancies. Following the arguments of Mott,²⁷ $\rho(0)$ more accurately may depend on the number of doubly occupied sites, which are quite different in the paramagnetic and spiral

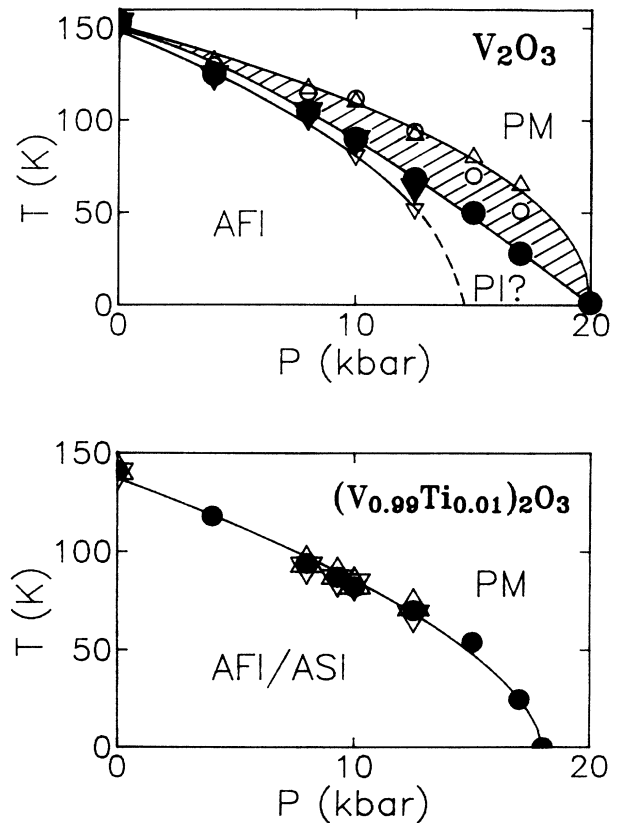


FIG. 8. Pressure-temperature phase diagrams for pure and Ti-doped V_2O_3 . PM, paramagnetic metal; PI, paramagnetic insulator; AFI, antiferromagnetic insulator; ASI, antiferromagnetic Slater insulator. The circles (triangles) correspond to signatures in the resistivity (susceptibility). The hatched region indicates a precursory magnetic region, presaging the metal-insulator transition.

spin-density wave states of compressed pure V_2O_3 and $V_{2-y}O_3$, respectively.

CONCLUSIONS

We summarize our data by graphing in Fig. 8 the P - T phase diagrams for stoichiometric V_2O_3 and $(V_{0.99}Ti_{0.01})_2O_3$. In the V_2O_3 phase diagram (derived from Figs. 5 and 7), the solid circles mark the temperature of the hysteretic jump in $\rho(T_{MI})$, which, for $P < 15$ kbar, coincides with the step in $\chi(T_N)$, denoted by the solid, down triangles. The antiferromagnetic insulator has an energy gap which can be described within the Mott-Hubbard picture in terms of the bandwidth B and the intra-atomic repulsion term U . The open up and down triangles bracket the (hatched) interval over which $\chi(T)$ changes smoothly, defining a precursory region to the transition with magnetic character. The onset of an upturn (open circles) in $\rho(T)$ in the metal, preceding a local maximum, overlays the high-temperature start of the drop in the susceptibility at low P , but decouples for $P \geq 15$ kbar. It is this part of the phase diagram where we observe unusual resistive behavior near the $T \rightarrow 0$ MIT. The resistivity has a magnitude and temperature dependence akin to that of the paramagnetic insulating (PI) phase which occurs for chromium-doped V_2O_3 .²⁸ The fact that $\rho(T)$ is hysteretic and its value remains

above the Mooij limit²⁹ favors a description as an insulator, but it is possible that the upper and lower Hubbard bands barely overlap, leading to a semimetal. In any case, the absence of both long-range magnetic order and substitutional disorder makes this sliver of the pure V_2O_3 P - T diagram a special one, with great promise for isolating the effects of strongly enhanced electron correlations at the MIT. The pressure-stabilized metal appears as well to remain a paramagnet, in contrast to the antiferromagnetic order which develops below $T \sim 10$ K in both the Ti-doped and vanadium deficient compounds.

The transport (circles) and magnetic (triangles) signatures of the transition (from Fig. 6) coincide for all P in $(V_{0.99}Ti_{0.01})_2O_3$. Here, the long-range magnetic order is robust under pressure. Moreover, the insulating state has a significant magnetic contribution to the energy gap, requiring a combination of the Mott-Hubbard description and the Slater formalism to account for $\Delta_a(P)$.

ACKNOWLEDGMENTS

The work at the University of Chicago was supported by the NSF Materials Research Laboratory under Grant No. DMR88-19860. S.A.C. acknowledges support from NSF Grant No. DMR92-04820. The work at Purdue University was supported under MISCON Grant No. DE-FG02-90ER45427.

*Present address: AT&T Bell Laboratories, Murray Hill, NJ 07974.

¹N. F. Mott, Proc. Phys. Soc. London, Ser. A **62**, 416 (1949); J. Hubbard, Proc. R. Soc. London, Ser. A **281**, 401 (1964).

²B. I. Shraiman and E. D. Siggia, Phys. Rev. Lett. **62**, 1564 (1989); C. Jayaprakash, H. R. Krishnamurthy, and S. Sarker, Phys. Rev. B **40**, 2610 (1989); C. I. Kane *et al.*, *ibid.* **41**, 2653 (1990).

³X. Y. Zhang, M. J. Rozenberg, and G. Kotliar, Phys. Rev. Lett. **70**, 1666 (1993); G. Vignale and M. R. Hedayati, Phys. Rev. B **42**, 786 (1990); V. Janis, J. Masek, and D. Vollhardt, Z. Phys. B (to be published).

⁴J. Spalek, M. Kokowski, and J. M. Honig, Phys. Rev. B **39**, 4175 (1989); J. Spalek, A. Datta, and J. M. Honig, Phys. Rev. Lett. **59**, 728 (1987).

⁵W. F. Brinkman and T. M. Rice, Phys. Rev. B **2**, 4302 (1970); Phys. Rev. Lett. **27**, 941 (1971).

⁶W. Bao *et al.*, Phys. Rev. Lett. **71**, 766 (1993).

⁷S. A. Carter *et al.*, Phys. Rev. B **48**, 16 841 (1993).

⁸Y. Tokura *et al.*, Phys. Rev. Lett. **70**, 2126 (1993).

⁹S. A. Carter *et al.*, Phys. Rev. Lett. **67**, 3440 (1991).

¹⁰D. B. McWhan, T. M. Rice, and J. P. Remeika, Phys. Rev. Lett. **23**, 1384 (1969); D. B. McWhan *et al.*, Phys. Rev. B **7**, 1920 (1973).

¹¹S. A. Shivashankar and J. M. Honig, Phys. Rev. B **28**, 5695 (1983).

¹²J. Dumas and C. Schlenker, J. Magn. Magn. Mater. **7**, 252

(1978).

¹³Y. Ueda, K. Kosage, and S. Kachi, J. Solid State Chem. **31**, 171 (1980).

¹⁴S. A. Carter *et al.*, Phys. Rev. B **43**, 607 (1991); T. F. Rosenbaum and S. A. Carter, J. Solid State Chem. **88**, 94 (1990).

¹⁵J. Feinleib and W. Paul, Phys. Rev. **155**, 841 (1967).

¹⁶J. C. Slater, Phys. Rev. **82**, 538 (1951).

¹⁷H. R. Harrison, R. Aragon, and C. J. Sandberg, Mater. Res. Bull. **15**, 571 (1980).

¹⁸S. A. Shivashankar *et al.*, J. Electrochem. Soc. **128**, 2472 (1981).

¹⁹N. F. Mott, Philos. Mag. **19**, 635 (1969); V. Ambagaokar, B. I. Halperin, and J. S. Langer, Phys. Rev. B **4**, 2612 (1972).

²⁰A. L. Efros and B. I. Shklovskii, J. Phys. C **8**, 249 (1975).

²¹P. D. Dernier and M. Marezio, Phys. Rev. B **2**, 3771 (1970).

²²K. E. Smith and V. E. Heinrich, Phys. Rev. B **38**, 5965 (1988).

²³A. Menth and J. P. Remeika, Phys. Rev. B **2**, 3956 (1970).

²⁴A. K. Mabatha *et al.*, Phys. Rev. B **21**, 1676 (1980).

²⁵P. C. Canfield, J. D. Thompson, and G. Gruner, Phys. Rev. B **41**, 4850 (1990).

²⁶P. C. Canfield, J. D. Thompson, S. W. Cheong, and L. W. Rupp, Phys. Rev. B **47**, 12 357 (1993).

²⁷N. F. Mott, *Metal-Insulator Transitions*, 2nd ed. (Taylor & Francis, London, 1990).

²⁸H. Kuwamoto, J. M. Honig, and J. Appel, Phys. Rev. B **22**, 2626 (1980).

²⁹J. H. Mooij, Phys. Status Solidi A **17**, 521 (1973).